

# Windsurf fin- numerical and experimental analysis of ultimate strength

*Francisco de Albuquerque Nascimento*  
*francisco7nascimento@gmail.com*  
*Instituto Superior Técnico, University of Lisbon, Portugal*  
*July 2017*

*Abstract*— The objective of this work is to analyze numerically and experimentally the ultimate strength of a windsurf fin, produced in composite materials. A FE model is developed and validated by a real scale-experiment. The FE analysis is performed using the commercial software ANSYS. The fin structure is analyzed, both in the linear and non-linear domain when subjected to remote load, applied at different locations of the structure, identifying the evolution of the stresses and the consequent deformation. Beyond the numerical model, it is also analyzed the structure in the laboratory, reproducing the load used in the computational analysis. The output of the numerical analysis is compared to the experimental one and calibrated. To determine the fin's stage of failure the Tsai-Wu failure criteria, which predicts only if exists or not breaks, independently the mode which the fin breaks is employed. Were also applied the Maximum Stress Criteria and the Maximum Strain Criteria to have predictions of the complete break of the fin.

*Key-Words*— ANSYS, Composite Materials, Finite Element Method, Tsai-Wu, Ultimate Strength

## 1. INTRODUCTION

The maritime market choice for composite is more and more attractive. It is now possible to construct composite structures which performs better than the metal ones, wherever we talk in terms of weight, strength or cost. To achieve this, it requires a good control of quality. It is also important that the designer and producer have a knowledge of fiber reinforced plastics (FRP) composite materials and associated mechanics. Composites offer the prospect of weight saving and low maintenance, as well as being non-magnetic. These advantages put the composite materials far ahead, when the shipyards must decide whether go to metallic or composite materials.

As materials and building practices improve, it is not unreasonable to consider composite construction for vessels up to 100 meters. Although design principles for ship structures and composite materials used in aerospace structures are mature as individual disciplines, procedures for combining the technologies are at an infancy [1].

Creation of valid numerical models is the only possible to predict the complex behavior of the materials, due to their anisotropic properties and multifaceted internal interactions. The finite element method analysis is an important tool in this sector. With the advance of powerful finite element (FE) models, the accuracy of the predictions gets higher and higher, enabling the shipyards to construct with more confidence and reducing the margin of error. The nautical sports sector is one of the areas where more investment is made to obtain better results, due to its high level of competition and the constant necessity of keeping in the vanguard of the expertise.

The application of finite element method to study the structural response of windsurf fins is still undeveloped,

making the margin of progression a motivation to address this area. The sector is reaching a point where the expertise of the shipyards requires numerical support to advance, to improve the performance and obtains better results. The know-how is getting overcome by the finite element application and in the nautical sports area this is getting more evident with the consequent introduction of FEM analysis in the design of every part or boat of the high level of competition. Windsurf area is not an exception, and the preliminary improvements are being obtained by the leading companies of the sector, showing the necessity of winning every competition, wherever talking about world championships or even the Olympics where this sport participates from 1984.

The windsurfing fin is one of the most important pieces in this sport. It is the board's pivot point, and plays a major role in the board's maneuverability. To understand this, it is necessary to think the fin as a wing in the water that is the same on both sides. As any wing, the fin is designed to allow pressure to flow from the side, and divert the pressure into forward thrust and lift [2].

To reduce trial and error fabrication processes, the implementation of Finite Element Method is an essential tool. The capacity of easily changing internal properties, shapes or other important aspects creation of numerical is obtained by creating numerical models, which can be tested and help to predict the structural response to the applied loads. For builders like F-Hot, who produces fins to world champions, it is essential to understand the structural behavior under hydrodynamic pressure loads during sailing. Due to the complex nature of the fin's structure with its stiffeners, piles of carbon and glass at various orientations, it would be difficult to predict the twist and flexure of the fin using standard hand calculations. The finite element model allows

the user to easily modify the composite lay-up of the fin to achieve the desired structural characteristics, achieving better results quicker and with less effort.

The Finite Element Method has become the most powerful instrument in structural analysis, allowing to analyze the strength of highly complex structures, wherever this complexity comes from its size or questions about the difficulty to predict of the response of composite materials.

Therefore, the scope of this work is to analyze a windsurf fin studying its ultimate strength, through a numerical model in FEM and experimentally in the laboratory of a real-scale fin.

## 1.2 Objectives

The principal objective is to create a numerical model of a windsurf fin, analyzing its ultimate strength. This numerical model is to be calibrated with the data obtained in the laboratory, where a real-scale model is to be tested.

The tests are going to be settled in two ways: Numerically, where the model is created to be analyzed in terms of stresses and deformations, applying after a failure criterion for composite materials; and experimentally, the fin is to be tested only in the linear-elastic domain, where the resulting values are going to be used in the numerical model to calibrate it, correcting the initial differences of the structural response after applying remote loads at different points of the structure.

This work is an important first step to further developments about the windsurf fin, allowing future FEM projects to start a step ahead.

## 2. COMPOSITE MATERIAL DESCRIPTORS

It is important to know the elastic properties of the laminate. One of the primary factors which determine the properties of composites is the relative proportions of the fiber's and matrix. The proportions can be in terms of weight or volume fractions. For theoretical analysis, volume fractions are better to obtain despite the weight fractions are easier to get during the construction process and experimentally [3].

Considering a case with weights/volumes of fiber's, matrix and net composite being  $w_f/v_f$ ,  $w_m/v_m$  and  $w_c/v_c$  respectively. Letters f, m and c are used to indicate fiber, matrix and composite respectively. Volume and weight fractions are denoted by V and W respectively[3]. So, for volumes:

$$v_c = v_f + v_m \quad (1)$$

$$V_f = \frac{v_f}{v_c}, V_m = \frac{v_m}{v_c} \quad (2)$$

and for weights:

$$w_c = w_f + w_m \quad (3)$$

$$W_f = \frac{w_f}{w_c}, W_m = \frac{w_m}{w_c} \quad (4)$$

Knowing these relations, the density of the composite it is established by:

$$\rho_c v_c = \rho_f v_f + \rho_m v_m \quad (5)$$

Dividing both sides by  $v_f$  and using the definitions of volume fractions,

$$\rho_c = \rho_f V_f + \rho_m V_m \quad (6)$$

Using the weight terms:

$$\rho_c = \frac{1}{\left(\frac{W_f}{\rho_f}\right) + \left(\frac{W_m}{\rho_m}\right)} \quad (7)$$

At this point, it is important to define FVF and FWF (fiber weight fraction). Starting with the fiber volume fraction from the fiber weight fraction:

$$FVF = \frac{1}{\left[1 + \frac{\rho_f}{\rho_m} * \left(\frac{1}{FWF} - 1\right)\right]} \quad (8)$$

With some mathematical transformations, it can obtain the fiber weight fraction of the fiber volume fraction [4]:

$$FWF = \frac{\rho_f * FVF}{\rho_m + [(\rho_f - \rho_m) * FVF]} \quad (9)$$

Like it can be easily observed, the two fractions depend one on each other, but the fiber weight fraction, as said before, can be calculated experimentally, knowing the mass of resin and matrix applied. So, the fiber weight fraction can be calculated as:

$$FWF = \frac{m_f}{m_f + m_m} \quad (10)$$

In terms of important definitions, there is one more that is going to be used in this project, which is, the cured ply thickness (CPT). This expression will give the thickness, in millimeters, of each ply, taking account the fiber area weight (WF) in grams per square meter, the fiber densities, expressed in grams per cubic centimeter and the fiber volume fraction for each type of fiber. So, the expression is going to be:

$$t = \frac{W_f}{\rho_f * FVF * 1000} [mm] \quad (11)$$

With these deductions, the values of the fibers, resin and the final laminate can be expressed as:

$$\rho_m = 1.2 \text{ g/cm}^3 \quad (12)$$

$$\rho_{e-glass} = 2.580 \text{ g/cm}^3 \quad (13)$$

$$\rho_{carbon-UD} = 1.5003 \text{ g/cm}^3 \quad (14)$$

$$\rho_{carbon-woven} = 1.47 \text{ g/cm}^3 \quad (15)$$

F-Hot used 97 grams of reinforcements (summing all the reinforcements used to produce one fin) and 140 grams of epoxy resin (matrix). In this way:

$$FWF = 40.92 \% \approx 41\% \quad (16)$$

and using Equation (8):

$$FVF_{carbon\_UD} = 39.56\% \quad (17)$$

$$FVF_{carbon\_woven} = 40.04\% \quad (18)$$

$$FVF_{e-glass} = 27.57\% \quad (19)$$

These values gave the ability to calculate the thickness of a ply of each type of reinforcement, using the Eqn (11):

$$t_{carbon-woven (100g/m^2)} = 0.170 \text{ mm} \quad (20)$$

$$t_{carbon-woven (200g/m^2)} = 0.374 \text{ mm} \quad (21)$$

$$t_{carbon-UD} = 0.169 \text{ mm} \quad (22)$$

### 3. FINITE ELEMENT MODEL

The numerical model was created using the commercial software ANSYS 18. When creating the finite element model, it was necessary to discretize the geometry, where the final one consists of 2597 nodes and 2610 elements, where most of them are quadrilateral, but to give a better cover to the curvature of the model, where the element size is from 2 to 10 millimeters, the software was forced to keep the element size between these values.

It was used the default element of ANSYS Workbench for shell elements, which is the SHELL181. This element is a four-node element with six degrees of freedom at each node: translations in the x, y, and z directions, and rotations about the x, y, and z axes. It is well-suited for linear, large rotation/deformation and large strain nonlinear applications.

After defining the mesh density, the ACP pre - processor was used, a specific part of the software for composites and to make the plies. The first one is mainly used to define the composite fabrics, define the element orientation (to properly orient materials), define the ply sequence for groups of elements. The second one is to analyze the results, having the ability to apply failure criteria specifically for composite.

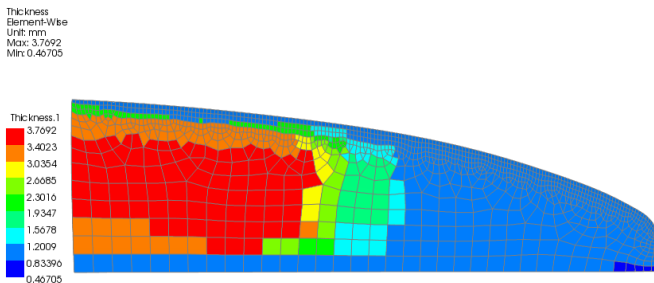


Figure 3.1- ACP Model Thickness

Figure 3.1 shows, from the top view, the thickness variation along the fin. As it can be observed, the region near the fixed support is going to be more filled with plies, due to the high stresses when the model is subjected to a local vertical force.

It is very important to understand the laminate of the fin, what plies are in there, what area do they occupy and what is the orientation of them. To comprehend this, Figure 3.2 traduces how is organized. This knowledge will lead to a better

comprehension of the results. In terms of representation, the figure only indicates half of the fin and the number of layers is organized from the outside to the inside. Both parts (named as *TOP* and *DOWN* for better organization during the project) are equal. In terms of tests, the *TOP* part will be under tension and the *DOWN* will be under compression.

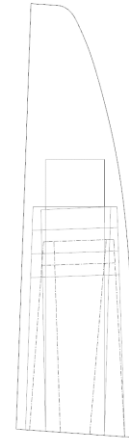


Figure 3.2- Layers Sketch

The lay-up of the fin included woven carbon and unidirectional carbon and glass reinforcements, but the exact lay-up schedule cannot be detailed here due to commercial considerations

After creating the fin, selecting the elements and all the properties, boundary condition of the FE was set (that it is going to be replicated in the set-up of the experimental test) to give the best approximation to the fin in relation to the box where the fin is fixed. The boundary condition was set as shown in.

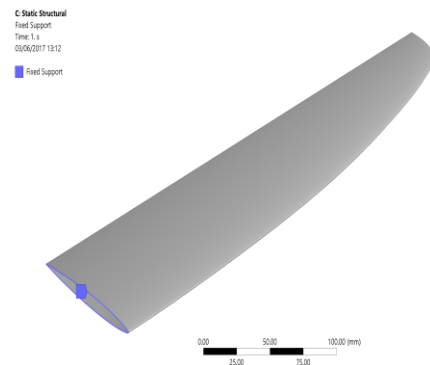


Figure 3.3- Boundary Condition in ANSYS

## 4. EXPERIMENTAL ANALYSIS

### 4.1 Set-Up

The fin was fixed with long bolts that went from the bottom of the structure until the fin's box, where, using nuts, the fin was tight, replicating the fixed support of the boundary condition. To make the test, it was used a hydraulic cylinder, fixed in the structure, above and perpendicular to the fin. The hydraulic system was controlled by a computer, where the

input was the displacement of the cylinder, in this case, downwards. Attached to the cylinder, it was used a round small indenter. It was used this, to ensure that the contact area was small, simulating a local force and it was not pointy to avoid marking permanently the fin. The possibility of slip due to large deformation was discharged because, to the point where the experience was made, the displacement was small and, both the fin and the indenter were fixed, so that possibility was liquidated.

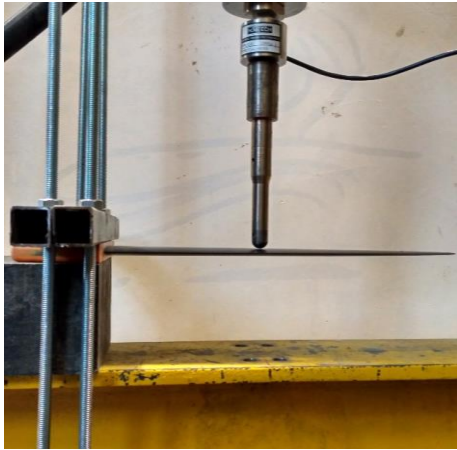


Figure 4.1- Experimental Set-Up

#### 4.2 Experimental Tests and Results

Two tests were made, both on the quarter cord line: first one at 80% span, in a point weaker where fewer values of force would imply greater values of displacement and other at 40%, in a point nearer the center of the gravity of the fin as it can be seen in Figure 4.2 (the nearest point from the tip wasn't used to make any experience). In both tests, it was used a deflection's speed of 0.1mm/s.



Figure 4.2- Fin with Loading Points Marked

The hydraulic cylinder was linked to a computer which stored the data (force and deflection at the loading point) of the test.



Figure 4.3- 40% Span Test



Figure 4.4- 80% Span Test

The consequent force-displacement data that came out of the tests are:

#### 40% SPAN TEST

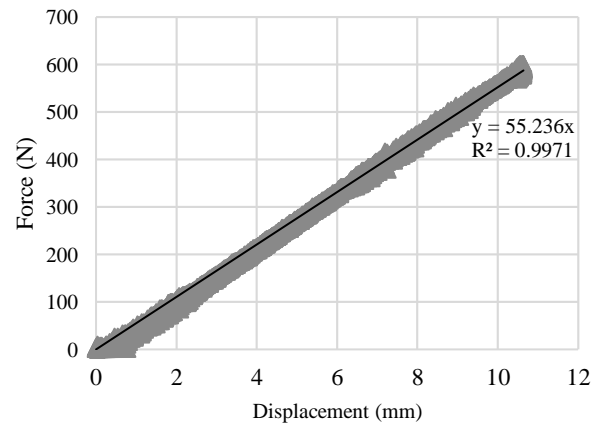


Figure 4.5- Force-Displacement Graphic (40% Span)

## 80% SPAN TEST

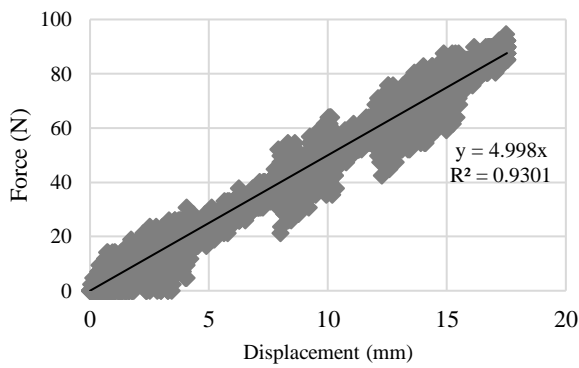


Figure 4.6- Force- Displacement Graphic (80% Span Test)

Figure 4.5 and Figure 4.6 indicates that the behavior of the fin is almost linear, showing that the fin's behavior is still in the elastic domain. This is also proved, by the returning to the initial position of the fin, when the forces took off, there is no permanent deformation. Another conclusion is that, due to a higher moment and even to be in a region in fewer plies, the 80% span test requires a lot less force to present much higher deformation.

### 4.3 Calibration Process

Knowing that the first values used from ANSYS library and from the report of Paul Miller [5] were rather different from the final ones, it is essential to understand how this development was made. After seeing the results, and comparing them with the previous predictions the force-displacement, it was decided that the model should be calibrated from the 40% span data, because it would be more trustable, due to the higher forces that could be applied, and due to small displacement/rotation in that point. In this way, the young moduli of the material properties that were used in input values were readjusted to give the model better results. Some other processes could be adopted but this one was selected in the way that, it was the easiest, quickest and the safest one.

There were three types of fibers that could be adjusted: unidirectional carbon fibers, multidirectional carbon fibers and unidirectional glass fibers. First, it was necessary to maintain the relation between the values and their respective directions, meaning that in the multidirectional fibers,  $E_x$  and  $E_y$  should have equal values and in the unidirectional ones,  $E_y$  and  $E_z$  were the ones that should be equal. A second important topic was that, in each fiber, the relation (increasing or decreasing in relation to the initial value) was made equally in all directions.

The initial input values were used to initiate the calibration process. In this way, the first simulation at 40% of span and a quarter of the chord from the leading-edge lead to the result shown at Figure 4.7.

## FORCE-DISPLACEMENT (40% SPAN)

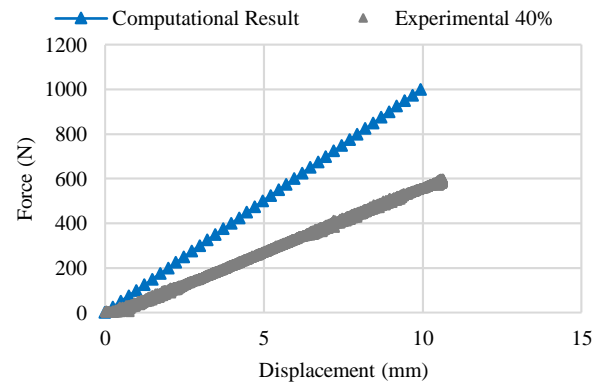


Figure 4.7- Graphic Force- Displacement (40% Span)- Experimental vs FEA Model with initial ANSYS Young Moduli values

This first approach indicates that the numerical model is more strength than it should be, compared with the real fin. In this way, it was necessary to reduce the values of the young moduli of the fibers, although this process needed to be taken with precaution to maintain the rigid structure of the fin. After some tests, one of the main conclusions was that, the plies that occupy more area of the fin, should be reduced less in order to maintain the linear behavior. This is even more evident because the e-glass fibers are displaced in a central region almost at 50% of the span. If this fiber had greater values compared to the carbon ones, it would lead to a break at the end of the e-glass fibers (this break would be completely unreal compared to the theoretical breaking point).

To calibrate the numerical model, all three values of young moduli were reduced and the final values were obtained by trial and error, maintaining the initial proportions and the relations concerning the type (unidirectional or multidirectional). The values can be observed in Table 4-1-Final Values of Young Moduli of the and the resulting comparison between the data obtained from the experimental tests and the behavior of the numerical model can be observed in Figure 4.8.

Table 4-1- Final Values of Young Moduli of the Fibers

	Units	Epoxy Carbon UD	Epoxy Carbon Woven	Epoxy E-Glass UD
$E_x$	MPa	58606	30670	12000
$E_y$	MPa	2413	30670	2668
$E_z$	MPa	2413	3450	2668

### FORCE- DISPLACEMENT (40% SPAN)

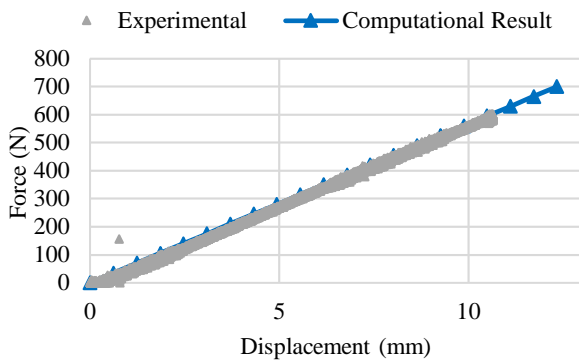


Figure 4.8- Graphic Force-Displacement (40% Span)- Experimental vs Computational

As it can be observed in Figure 4.8, the numerical model follows up closely the behavior of the real fin, demonstrating that the model created in ANSYS is trustable, although safety margins are always required. With this first verification, it is necessary to verify if the large deformation option could be turned off in ANSYS. This is usually a major source of problems, giving, in most of the times, problems of convergence and, as results, problems in the accuracy of the results.

Moment-Curvature analysis is a method to determine the load-deformations behavior of a concrete section using nonlinear material stress-strain relationships. For a given axial load, exists compression fiber strain and a section curvature  $\phi$  at which the nonlinear stress distribution is in equilibrium with the applied axial load. A unique bending moment can be calculated at this section curvature from the stress distribution [6]. The resulting moment-curvature relation is shown in Figure 4.9.

### MOMENT-CURVATURE

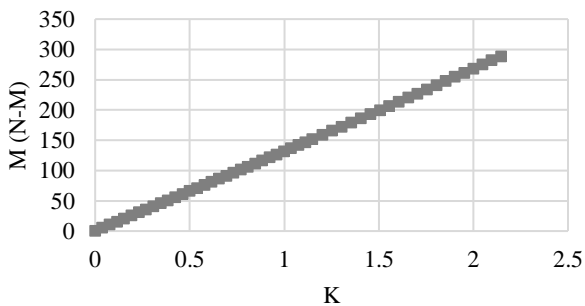


Figure 4.9- Moment- Curvature

$$k = \frac{1}{\rho} = \frac{d\theta}{ds} \quad (23)$$

Considering B as the application point of the force, A the fixed support point:

$$d\theta \approx \Delta\theta = \theta_B - \theta_A = \theta_B - 0 = \theta_B \quad (24)$$

and

$$ds \approx \Delta s = \sqrt{(x_B - x_A)^2 + (v_B)^2} \quad (25)$$

Converting Eqn (23) into:

$$k = \frac{\theta_B}{\sqrt{l^2 + v_B^2}} \quad (26)$$

where  $v_B$  is the vertical deflection in the application point,  $\theta_B$  is the rotation (in radians) at point B and  $l$  is the longitudinal distance from point A to B.

In terms of deformation, it is expected that the maximum deformation occurs in the tip of the fin. In this case, Figure 4.10 shows de deformation for 1000N. It is represented also the non-deformed shape.

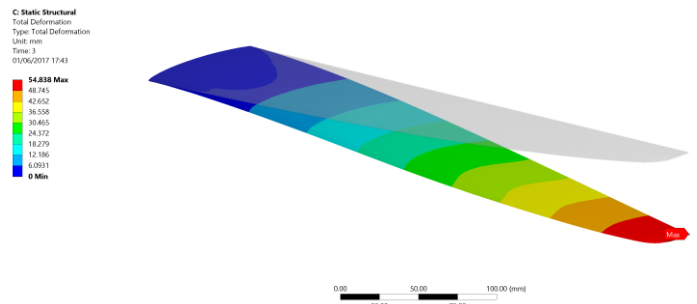


Figure 4.10- Deformation (1000N)

Distribution of the stresses needs to be analyzed. Due to its fixed support, it is expected to have higher stresses near the support. Figure 4.11 is representative of a 1000N load applied and are represented the maximum principal stresses.

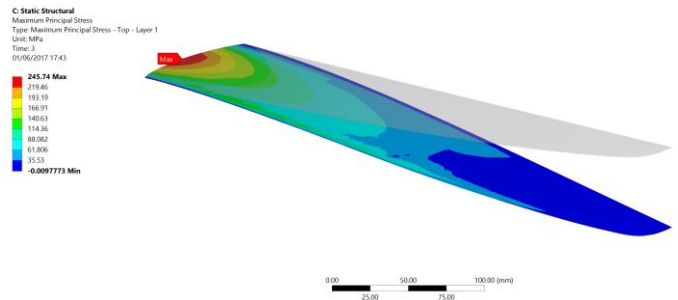


Figure 4.11- Distribution of Maximum Principal Stresses (1000N)

Higher stresses occur near the fixed support, where the fin concentrates most of its stresses. These results can lead to an estimate that, when the fin will break, it should be near the support, due to the accumulation of stresses that will lead to a complete failure.

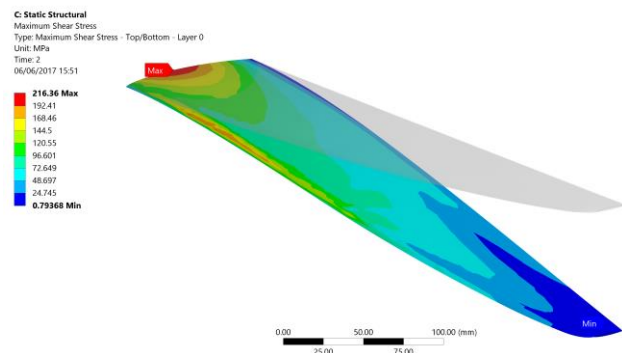


Figure 4.12- Distribution of Shear Stresses (1500N)

One of other important stresses that need to be analyzed is the shear stress. It is represented the distribution of shear stresses when applying a load of 1500N in Figure 4.12. These shear stresses are not the interlaminar shear stresses, but are the ones induced by the vertical remote force.

## 5. FAILURE ANALYSIS

Most experimental determinations of material strength, properties are based on uniaxial tests. Despite this, when we are talking about composite structures, multi-axial stress states are present and it is very important to predict the failure in all these different stress states [7]. Although it is necessary to prevent this multi-axial stress states, it is also very important to analyze the type of materials that are used in the composite structures. In this way, most of the materials used are anisotropic. These anisotropic materials are materials whose properties are directionally dependent, which is the complete opposite to the isotropic materials, where the material properties are equal despite the orientation. This characteristic is one of the major sources of errors between the computational models and the real ones because the shipyards develop their own ways to apply the fibers and resins, and the final properties will change, leading to different results in the propagation of the stresses and the consequent deformations [8].

Tsai-Wu [9] created a strength criterion for composites is that there exists a failure surface in the stress space in the following scalar form:

$$f(\sigma_k) = F_i \sigma_i + F_{ij} \sigma_i \sigma_j = 1 \quad (27)$$

where the indexes  $i, j, k=1, \dots, 6$  are used in a 3D case (repeated indexes imply summation); and  $F_i$  and  $F_{ij}$  are second and fourth rank tensors, respectively. The higher order terms  $F_{ijk} \sigma_i \sigma_j \sigma_k$  were ignored, because it is not practical from the operational point of view and cubic terms would make the failure surface open-ended. In relation to the terms, the linear one  $\sigma_i$  considers internal stresses showing the difference between positive and negative stress-induced failures. The quadratic terms  $\sigma_i \sigma_j$  are the ones who define the ellipsoid in the stress-space.

After some mathematical manipulation and assuming orthotropic case, Eqn (27) can be written as:

$$F_1 \sigma_1 + F_2 \sigma_2 + F_{11} \sigma_1^2 + 2F_{12} \sigma_1 \sigma_2 + F_{66} \sigma_6^2 = 1 \quad (28)$$

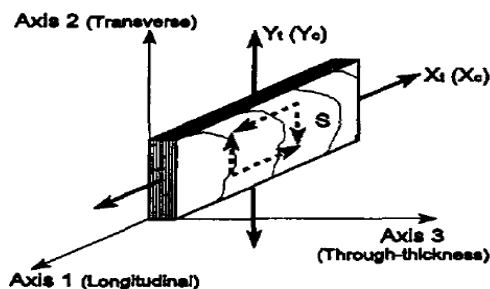


Figure 5.1- Plane Stress State [10]

Considering Figure 5.1, the five principal strengths are tension and compression parallel to the direction of the fiber ( $X_t$  and  $X_c$ ), tension and compression transverse to the direction of the fiber ( $Y_t$  and  $Y_c$ ), and shear in the same plane ( $S$ ).

A sample of the resulting stress-space case with this failure criterion is:

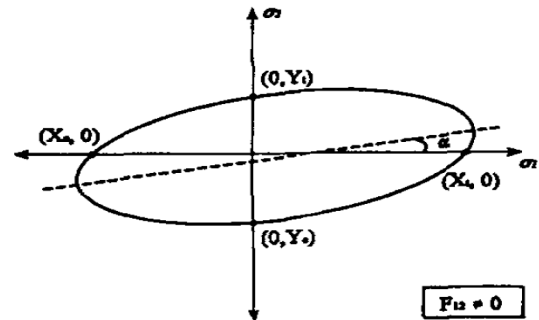


Figure 5.2- Sample Tsai-Wu Failure Surface [10]

The surface forms an ellipsoid in stress space, where  $F_{12}$  characterizes the rotation ( $\alpha$ ) of the ellipsoid with respect to the stress coordinate axis. Assigning  $F_{12}$  to zero is acceptable for filamentary composites [11]. This criterion cannot predict the type of failure, which for this work, is not relevant. In this main group of failure criteria not associated with the failure modes, the Tsai-Wu it is one of the most important ones [12].

## 5.2 Application

Applying the Tsai-Wu criterion, it was necessary to search for the value where a ply presents a value over one as stated in Equation (28). After the search, the value of the force that produces a first ply failure is 910N in the 1<sup>st</sup> ply that is under compression, showing a factor above 1 (1.0307), which indicates failure.

Ply-Wise  
Set: 27 - Time/Freq: 2.7  
Max: 1.0307  
Min: 0.011823  
Selection:  
AP - P1L1\_1.DOWN

Tsai-Wu Criteria  
1.0307  
0.92879  
0.8269  
0.72502  
0.62313  
0.52125  
0.41936  
0.31748  
0.21559  
0.11371  
0.011823

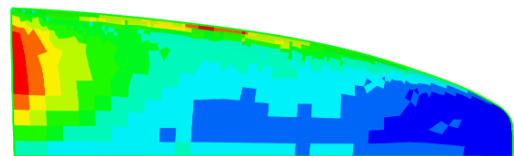


Figure 5.3- Tsai-Wu Failure

Higher values are near the fixed support. It is also observed a higher stress small region near the leading edge at the half of the span, but that should be ignored because it is possible to be due to a modelling error.

Although Tsai-Wu criterion presents trustable values, does not tells what kind of failure occurs. Knowing that information is not the most important in the goals of the project, the possibility to have a prediction of a failure criteria associated with the failure modes, is way to understand better the real behavior of the fin. These criteria consider that the non-homogeneous character of composites leads different

failure modes of the constituents. The criteria are established using mathematical expressions, considering material strengths and strains limits. The criteria that are going to be analyzed are the Maximum Stress Criterion and Maximum Strain Criterion. Three different conditions of failure are considered, although in this project is only going to be analyzed the failure of the fibers [13]:

$$\text{Fibre: } \sigma_1 \geq \sigma_{1T}^u \text{ or } |\sigma_1| \geq \sigma_{1C}^u \quad (29)$$

$$\text{Matrix: } \sigma_2 \geq \sigma_{2T}^u \text{ or } |\sigma_2| \geq \sigma_{2C}^u \quad (30)$$

$$\text{Shear: } |\sigma_{12}| \geq \sigma_{12}^u \quad (31)$$

Studying the fiber failure, the values of the required force are, necessarily, higher. The results, proved this, explicating that the necessary force was 2050N, where the failure factor is above 1 (1.018), also near the fixed support part of the fin, like expected. This occurs in the compressive part of the fin (specifically in 4.DOWN ply).

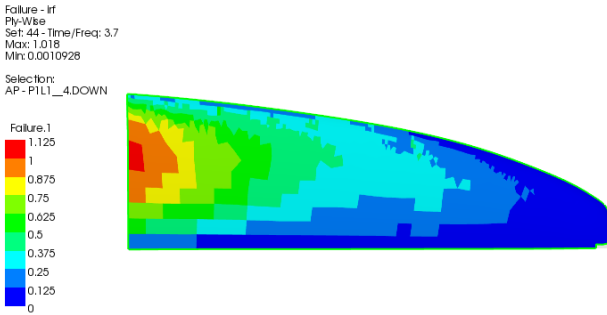


Figure 5.4- Fiber Failure- Maximum Stress Criterion

Moving to the second criterion: Maximum Strain Criterion. It is considered that the composite fails when the strain exceeds the respective allowable, being also a simple and direct way to predict failure of composites. Again, three different conditions are considered in correspondence with a maximum strain fiber direction, matrix or transversal direction and for shear strains:

$$\text{Fibre: } \varepsilon_1 \geq \varepsilon_{1T}^u \text{ or } |\varepsilon_1| \geq \varepsilon_{1C}^u \quad (32)$$

$$\text{Matrix: } \varepsilon_2 \geq \varepsilon_{2T}^u \text{ or } |\varepsilon_2| \geq \varepsilon_{2C}^u \quad (33)$$

$$\text{Shear: } |\sigma_{12}| \geq \sigma_{12}^u \quad (34)$$

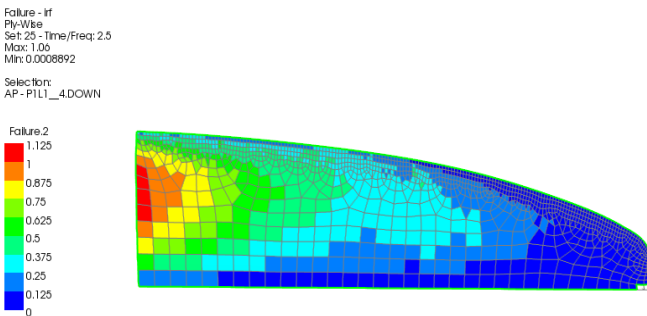


Figure 5.5- Fiber Failure- Maximum Strain Criterion

Figure 5.5 displays that the failure occurs also in the compressive side (ply 4.DOWN) when the force reaches a value of 825 N.

Resuming all these failure criteria values (not including the combined of maximum stress and strain criterion), relating the forces, deflections and maximum stresses in one single table:

Table 5-1- Failure Criteria Values

Failure Criterion	Force (N)	Ply Failure	Maximum Deflection (mm)	Maximum Stress (MPa)
Tsai-Wu	910	1.DOWN	49.902	223.62
Max Stress	2050	4.DOWN	109.68	393.18
Max Strain	825	4.DOWN	40.031	201.51

Analyzing the values, the first failure criterion that is full-filled is the maximum strain. This indicates that the fibers start to stretch more that they should but, despite this, the great difference between this value and the maximum stress values indicate also that it could be the data of the maximum strain values of the materials that it is not properly fit to the reality of the fin. This would be good values if we were analyzing the failure in the matrix, that requires much lower values to fail, as the Tsai-Wu failure criterion seems to indicate. This criterion is achieved with a relatively low value of force, which naturally indicates that the failure is in the matrix (although this is only a prediction since Tsai-Wu criterion does not indicate what is the failure mode as explained before).

Table 5-1 also demonstrates that, all criteria shows failure in plies that are under compression. This result is expected, since, when analyzing the orthotropic stress limits, the values that are for tension are (in absolute value) higher than the compression ones. Equal plies, subjected to the same forces in the same conditions, the compression ones will fail first because they have lower values of stress limits.

## 6. CONCLUSIONS

The objectives of this project were “to create a finite element model of a windsurf fin, analyzing its ultimate strength. This model was calibrated by the data obtained from the laboratory, where a real-scale specimen was tested.

The objectives were completed during the working process, wherever talking of the initial research, the creation of the finite element model, the experimental tests, the consequent calibration or the predictions of the failure of the fin.

Although the project does not have a large domain of results, this is explained by being a first and innovative work in this area, with the necessity of exploring much more before having the results. The development of a trustable computational model, to be used in further projects was one of the most important parts of this project. For this to happen, it was necessary to talk with some experts in composites, research and even with all this knowledge, it was necessary to adjust the FE model. In the composite area, information like material properties is not very spread, making the experience and internal knowledge a well-kept secret, but also making very difficult to advance in this type of projects.



The results of displacement were very accurate, with the model created in ANSYS 18 Workbench retrieving values of deformation very close to the ones obtained in the experimental test, showing a highly linear performance, predicting a very short plastic domain until the fin breaks.

In the failure modes, the application of the different criteria is very important to understand that the fail can occur in very different ways. The Tsai-Wu failure criterion cannot predict what is the failure mode but, due to its low value of failure mode, it is more probable that is associated with the cracks in the matrix (resin) because, when analyzing the failure of the maximum stress of the fibers, the values of the force are much higher than the ones presented by the Tsai-Wu criterion.

The innovative application of the FEM analysis to the nautical sport bodies in composites has an enormous space of development, making this the first work in the domain of the analysis of a windsurf fin in CENTEC. This first approach, with the model of the fin done and calibrated, allows the future works to move faster and deeper, moving ahead to other important domains.

The creation of a valid and calibrated numerical model, capable of predicting the structural behavior of the fin is the powerful tool in future studies. In terms of future work hypothesis, it would be very important to make an experimental test until the fin breaks. This would give a complete analysis of the behavior. This test would also give data about its plastic domain, that, although the predictions indicated a very small plastic domain, it would be important to confirm the predictions with experimental tests. It would be also interesting to make tests of dynamic loads, to adjust the model to a real fin, due to the fact that the fin is in constant changes of the direction so the loads are not even quasi-static. The disposition of the plies and even the type of the fibers applied could be also tested, applying different fabrics, changing the lay-up disposition and comparing the results to obtain the optimized model in terms of the structural response.

## 7. REFERENCES

- [1] E. Greene, *Marine Composites Second Edition*. 1999.
- [2] A. Raby, "Choosing Your Windsurfing Fin." p. 3, 2011.
- [3] R. A. Sheno and J. F. Wellicome, *Composite Materials in Maritime Structures, Volume 1 Fundamental Aspects*. Southampton, 1993.
- [4] Gurit Holding AG, "Guide to Composites." p. 74, 2000.
- [5] P. Miller, "NNS composite materials properties database, unpublished composite test program report," 1991.
- [6] F. Beer, E. R. Johnston, and J. T. Dewolf, *Mecânica dos Materiais*, 3th ed. Lisboa: McGraw Hill, 2003.
- [7] W. Van Paeppegem and J. Degrieck, "Calculation of Damage-dependent Directional Failure Indices from the Tsai-Wu Static Failure Criterion," *Compos. Sci. Technol.*, vol. 63, no. 2, pp. 305–310, 2003.
- [8] R. M. Christensen, "Failure Criteria for Anisotropic Fiber Composite Materials," 2008.
- [9] S. W. Tsai and E. M. Wu, "A General Theory of Strength for Anisotropic Materials," *J. Compos.*

- Mater.*, vol. 5, no. January, pp. 58–80, 1971.
- [10] P. Clouston, F. Lam, and J. D. Barrett, "Interaction Term of Tsai-Wu Theory for Laminated Veneer," *J. Mater. Civ. Eng.*, vol. 10, no. May, pp. 112–116, 1998.
- [11] R. Narayanaswami and H. M. Adelman, "Evaluation of the Tensor Polynomial and Hoffman Strength Theories for Composite Materials," *J. Compos. Mater.*, 1977.
- [12] P. Camanho, "Failure criteria for fiber-reinforced polymer composites," *Demegi, FEUP*, pp. 1–13, 2002.
- [13] P. P. Camanho, A. Arteiro, A. R. Melro, G. Catalanotti, and M. Vogler, "Three-dimensional invariant-based failure criteria for fiber-reinforced composites," *Int. J. Solids Struct.*, vol. 55, pp. 92–107, 2015.